Materials Research. 2016; 19(Suppl. 1): 92-96
DOI: http://dx.doi.org/10.1590/1980-5373-MR-2016-0290

The Effect of Cr Content on the Glass Forming Ability of $Fe_{68-x}Cr_xNb_8B_{24}$ (x =8,10,12) Alloys

Marcio Andreato Batista Mendes[a]*, Ana Karla Melle[b], Carlos Alberto Caldas de Souza[c], Claudio Shyinti Kiminami[b], Régis Daniel Cava[b], Claudemiro Bolfarini[b], Walter José Botta Filho[b]

[a] *Departamento de Engenharia de Materiais, Universidade Federal Tecnológica do Paraná – UTFPR, Av. dos Pioneiros, 3131, CEP 86036-370, Londrina, PR, Brasil*
[b] *Departamento de Materiais, Universidade Federal de São Carlos – UFSCAR, São Carlos, SP, Brasil*
[c] *Departamento de Ciência e Tecnologia dos Materiais, Universidade Federal da Bahia – UFBA, Salvador, BA, Brasil*

Received: April 9, 2016; Revised: September 10, 2016; Accepted: October 2, 2016

Based on the $Fe_{60}Cr_8Nb_8B_{24}$ alloy, reported in the literature as good Glass Forming Ability (GFA), in this study the GFA of two new compositions was proposed, $Fe_{68-x}Cr_xNb_8B_{24}$ (x=10,12). They were evaluated as good candidates to be new compositions of Bulk Metallic Glasses (BMG) with better corrosion resistance due to the high Cr content. Rapidly solidified glassy ribbons were processed, and based on their thermal characteristics, the critical thickness of the glassy structure formation (Zc) was estimated. The critical thickness (Zc) obtained experimentally using the wedge-shaped casting method was evaluated and it presented a much lower value than that estimated theoretically. However, the GFA of the compositions analyzed was ranked and this ranking (i.e. whichever has the most or least GFA) is in agreement with the result predicted theoretically. The GFA of $Fe_{58}Cr_{10}Nb_8B_{24}$, which presented a maximum thickness of the amorphous region of wedge-shaped samples of about 0.6 mm (but estimated it would be 3.56 mm), offered good prospects to be a new Fe-based glass former alloy which has better resistance to corrosion than the $Fe_{60}Cr_8Nb_8B_{24}$ alloy reported.

Keywords: *Bulk metallic glasses, Glass forming ability, Rapid-solidification processing, Fe-based alloys*

1. Introduction

Over the last few years, extensive research has been carried out to improve the properties of metallic glasses, such as the physical, chemical, magnetic and mechanical properties. The corrosion behavior of Bulk Metallic Glasses (BMG) is important when these materials are used in aggressive and hostile environments (high temperatures, oxidizing atmospheres and corrosive media)[1]. In Fe-based alloys, adding some elements such as Cr is known to improve the corrosion resistance of theses alloys, however it also reduces the Glass Forming Ability (GFA)[2]. The percentage of Cr in the glass former alloy could be lower than that of stainless steel as only 2% is sufficient to be resistant to pitting and crevice corrosion. In 1 N HCl solutions, the $Fe_{67.6}C_{7.1}Si_{3.3}B_{5.5}P_{8.7}Cr_{2.3}Mo_{2.5}Al_{2.0}Co_{1.0}$ alloy containing 2.3 at% Cr showed a corrosion resistance similar to the 304 stainless steel that contains high Cr (19 at% Cr) and Ni (9 at% Ni) contents[3]. This behavior indicates a promising replacement of stainless steel alloys by glassy alloys in various applications.

Despite the fact that Cr reduces the GFA of the alloy, it has been reported in the literature that a Fe-based BMG can be obtained containing up to 15 at.% Cr and 16 at.% Cr[4,5,6,7,8] and the corrosion resistance can be significantly improved due to this higher amount of Cr.

Besides Cr, molybdenum and niobium additions have also been extensively studied because both are also effective in promoting anodic passivation (similar to what happens to Cr), even in acidic chloride solution[2]. Kiminami et al. reported that a small quantity of Nb and/or Mo, lower than the minimum concentration generally used in commercial stainless steel (0.6 wt.%), is sufficient to increase the general corrosion resistance, as well as the pitting corrosion resistance of glassy Fe-Cr-based alloys[9]. It has been shown that Mo is more effective in enhancing corrosion resistance than the Nb in 4.0 M HCl solution, and the alloy containing both Nb and Mo presented more overall corrosion resistance than the alloy containing only one of these elements[10]. Furthermore, the presence of these two elements favors the increase in the GFA of the alloy.

Regarding the design and selection of compositions in Fe-based BMG with additions of Cr, Nb and B elements, Cheney and Vecchio[11] reported a modeling criterion that simultaneously analyzes the thermodynamics and kinetics of the vitrification behavior in a potential glass-forming alloy. The authors used a liquidus model (parameter α) to determine and rank the presence of deep eutectics. Moreover, this model was cross-checked with an elastic strain model (parameter ε) in a pseudo-ternary phase diagram. The authors analyzed 19 samples of this Fe-Cr-Nb-B system, and both theoretical

* e-mail: marciomendes@utfpr.edu.br

and experimental results showed that one of the optimal compositions is the $Fe_{60}Cr_8Nb_8B_{24}$. However, the authors did not consider the compositions with a high percentage of both Cr and Nb, which can offer better resistance to corrosion.

To analyze the liquidus temperature calculations, a dimensionless parameter, α, is used to quantify the depth of the eutectic, where a high value of alpha means a potentially good glass-forming alloy[11,12]. The parameter α is described by Eq. (1), where x_i is the atomic percent of the *i*th element and T_l is the liquid temperature of the alloy.

$$\alpha = \frac{\sum_{i=1}^{n} x_i T_i}{T_l} \quad (1)$$

The parameter ε, which calculates the elastic strain energy that must be stored in an emerging crystalline nucleus, is described in ref. 5. This elastic strain criterion states that the mean local strain must exceed 0.054 in order to destabilize the crystal lattice formation and encourage amorphization[11,12].

Based on these modeling criteria and on the $Fe_{60}Cr_8Nb_8B_{24}$ alloy reported by Cheney and Vecchio[11] as a good GFA, for this study the $Fe_{68-x}Cr_xNb_8B_{24}$ (x=10,12) compositions were considered as candidates to be new compositions of BMG with higher corrosion resistance due to the higher Cr content. It can be observed that these compositions have the desirable conditions established by Cheney and Vecchio[11], i.e., high value of alpha, ε > 0.054 and a chemical short range order parameter (CSRO)< (-0.04). A Nb concentration above 8 at.% was not used because it reduces the GFA[11]. Concerning the B element, a concentration above 24 at.% slightly increases the GFA[11], thus it was maintained at this concentration as the $Fe_{60}Cr_8Nb_8B_{24}$ alloy. Thus, in order to increase the Cr, it was decided to decrease the Fe content and not the B one because it favors the GFA[4].

This paper analyzes the effect of the increase in the Cr content on the structure and thermal stability of $Fe_{68-x}Cr_xNb_8B_{24}$ (x=10,12) alloys. For the sake of comparison, the $Fe_{60}Cr_8Nb_8B_{24}$ alloy reported by Cheney and Vecchio was also evaluated in this work.

2. Experimental Procedures

The $Fe_{68-x}Cr_xNb_8B_{24}$ (x=8,10,12) alloy ingots were produced by arc-melting the pure elements under an argon atmosphere. Rapidly solidified ribbons, approximately 1.4 mm wide and 45 μm thick were produced from the ingots, using a single-roller melt spinner at a tangential wheel speed of 40 m/s in an argon atmosphere. Bulk wedge-shaped samples with 0.5 μm up to 5 mm thick and 40 mm long were produced by the suction casting method in a copper mold. The samples were structurally characterized by X-ray diffraction (XRD) with Cu-Kα radiation and scanning electron microscopy (SEM). The liquidus temperature (T_l) of the alloys and the thermal stability of the glassy samples were evaluated using differential scanning calorimetry (DSC) and differential thermal analysis (DTA) at a heating rate of 0.67 K/s under a flowing Ar atmosphere.

3. Results and Discussion

Figure 1 presents the thermograms of the as-quenched ribbon. The arrows in Figure 1a indicate the glass transition temperature (T_g) and the crystallization temperature (T_x), and the arrows in Figure 1b indicate the liquidus temperature (T_l). These measured thermal parameters (T_g, T_x and T_l), and the calculated ΔT_x (supercooled liquid region, $\Delta T_x = T_x - T_g$), γ parameter ($T_x/(T_g+T_l)$)[13] and Z_C (critical thickness of the composition calculated using the relationship Z_c=2.80e(−7) exp (41.70γ))[13] are summarized in Table 1. According to Lu and Liu[13], γ values for BMGs vary from 0.350 to 0.500, therefore it would be possible to obtain a BMG with these alloy compositions, and it is theoretically possible to obtain an amorphous structure up to 3.5 mm for the $Fe_{58}Cr_{10}Nb_8B_{24}$ alloy and up to 1.6 mm for the $Fe_{56}Cr_{12}Nb_8B_{24}$ alloy. The $Fe_{60}Cr_8Nb_8B_{24}$ alloy obtained a higher ΔTx (=60 K) and Z_C (=4.35 mm) value than that reported by Cheney and Vecchio (ΔT_x=55 K and Zc=3.44 mm)[11].

Figure 2 shows the X-ray diffraction patterns of the as-quenched ribbons. It can be observed that all the alloys have a halo without any peaks, which is a characteristic of an amorphous structure, i.e. indicating that there was a formation of an amorphous structure. Despite these XRD results for the $Fe_{56}Cr_{12}Nb_8B_{24}$ alloy, Figure 3b shows the SEM micrograph in which the crystalline phases can be observed in the cross-section of the ribbon at a quantity that the XRD certainly did not detect. The SEM micrograph of the melt-spun $Fe_{58}Cr_{10}Nb_8B_{24}$ ribbon showed no evidence of crystalline phases, as shown in Figure 3a. This result, which showed higher GFA of $Fe_{58}Cr_{10}Nb_8B_{24}$ compared with $Fe_{56}Cr_{12}Nb_8B_{24}$, was predicted by the γ parameter (0.39 and 0.37 respectively) and by the critical thickness Z_C (3.56 and 1.63 mm respectively), as presented in Table 1.

The low tendency of the GFA of the $Fe_{56}Cr_{12}Nb_8B_{24}$ alloy is attributed to the high Cr content. Nevertheless, in the literature, cases can be found reporting BMG for alloys with a high Cr content, such as in the $Fe_{43}Cr_{16}Mo_{16}C_{10}B_5P_{10}$ (at%)[5] and $Fe_{43}Cr_{16}Mo_{16}C_{15}B_{10}$ (at%)[7] alloys, and this behaviour has been attributed to the high Mo content in these alloys, which is favorable in terms of increasing the GFA[14]. Moreover, in these alloys, the partial substitution of B by C and/or P also helps to increase the GFA[5].

The $Fe_{58}Cr_{10}Nb_8B_{24}$ alloy bulk sample, which has a thickness as high as 45 mm processed by the suction casting method, was analyzed by SEM. Figure 4a shows the SEM micrographs of a region (thickness around 1.0 mm) where some crystallized phases in the wedge-section of the $Fe_{58}Cr_{10}Nb_8B_{24}$ alloy can be observed. In this region, the microstructure consists of a few crystalline phases embedded

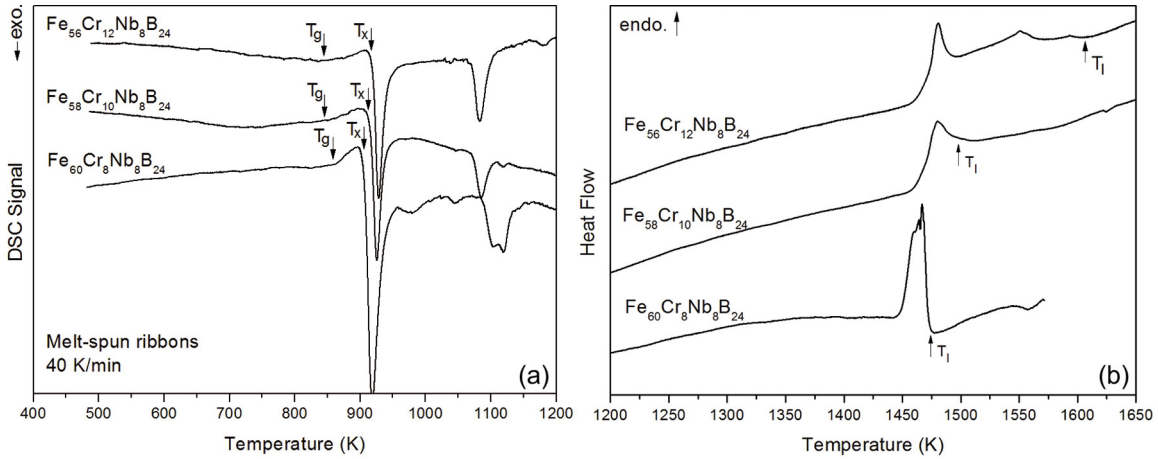

Figure 1: (a) DSC thermograms for as-quenched ribbon. Arrows indicate glass transition temperature (T_g) and crystallization temperature (T_x); (b) DTA scans for the glass-forming alloys. Arrows indicate liquidus temperature (T_l).

Table 1: Thermal characteristics of as-quenched ribbon and calculated critical thickness for glassy structure formation (Z_C).

Alloy	T_g (K)	T_x (K)	ΔT_x (K)	T_l (K)	γ	Z_C (calc.) (mm)
$Fe_{56}Cr_{12}Nb_8B_{24}$	845	916	71	1607	0.37	1.63
$Fe_{58}Cr_{10}Nb_8B_{24}$	832	914	82	1498	0.39	3.56
$Fe_{60}Cr_8Nb_8B_{24}$(*)	870	930	60	1472	0.40	4.35

(*) composition reported by Cheney and Vecchio[11].

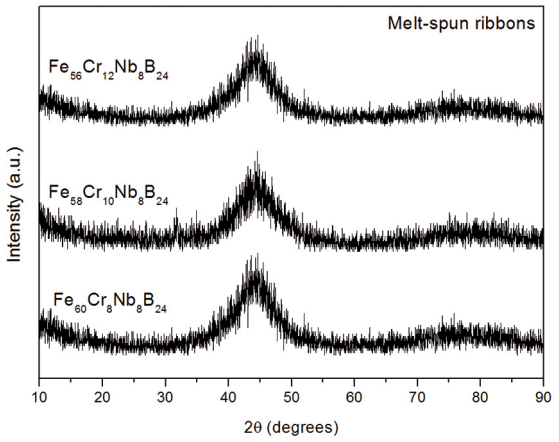

Figure 2: X-ray diffraction patterns for selected Fe-Cr-Nb-B alloys as-quenched ribbon.

in an amorphous matrix (featureless region). Figure 5 shows the X-ray diffraction patterns of three different regions of this sample (with 0.6 mm, 1.0 mm and 3 mm thicknesses). The diffraction pattern shows a fully glassy structure of 0.6 mm thickness and this is in agreement with Figure 4, where it can be observed that the early crystallized phases appear in the range of 0.6 to 1.0 mm. Combining the SEM and XRD analysis, the experimental critical thickness, Z_C, of around 0.6 mm for $Fe_{58}Cr_{10}Nb_8B_{24}$ alloy is lower than that theoretically predicted (3.56 mm as shown in Table 1).

For the $Fe_{60}Cr_8Nb_8B_{24}$ alloy, the same procedure of characterization of the bulk sample was performed by XRD and SEM. Combining the SEM and XRD analysis, the experimental critical thickness (Z_C) achieved was approximately 1 mm for this alloy, which is lower than that

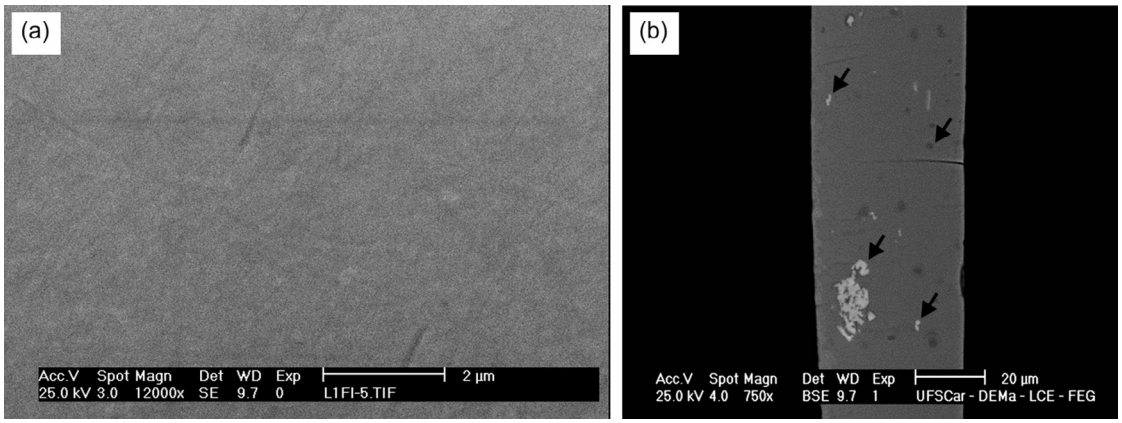

Figure 3: Scanning electron microscopy (SEM) images of cross section of the (a) $Fe_{58}Cr_{10}Nb_8B_{24}$ and (b) $Fe_{56}Cr_{12}Nb_8B_{24}$ alloys as-quenched ribbon.

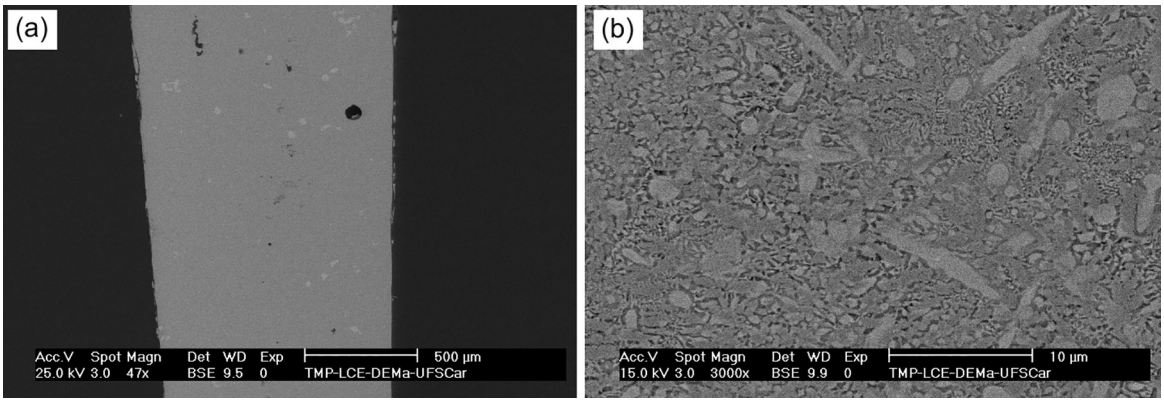

Figure 4: (a) Scanning electron micrograph (BSE) showing the critical thickness for the wedge specimen of $Fe_{58}Cr_{10}Nb_8B_{24}$ alloy; (b) morphology of the crystallized phases.

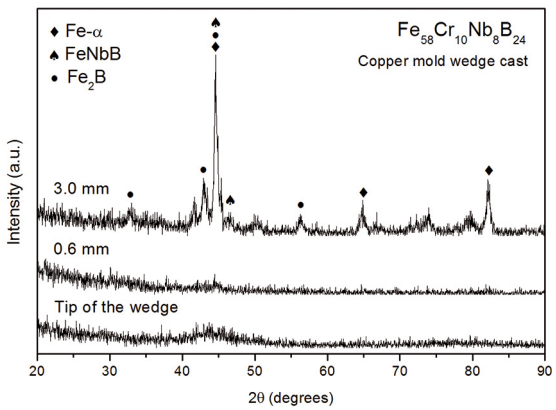

Figure 5: X-ray diffraction patterns of samples extracted from regions of different thicknesses of a copper mold wedge cast alloy.

theoretically predicted in this paper (4.35 mm as shown in Table 1) and also lower than that theoretically predicted by Cheney and Vecchio (3.4 mm)[11].

Studies to determine the experimental critical thickness by using the bulk wedge-shaped casting method, as seen in this paper, is widely used in this field of research. Nevertheless, the reproducibility of this method is a challenge, as reported by Sanders et al.[15], where the experimental critical thickness for $Al_{86}La_5Ni_9$ alloy reported was 685±95 µm after processing three samples. In view of this, the critical thicknesses for the Fe-Cr-Nb-B presented here might be higher, by improving the experimental procedures such as optimizing the alloy preparation and processing parameters. Therefore, the three compositions considered in this paper were ranked and this is in agreement with that predicted theoretically: the GFA decreases with increasing Cr content.

4. Conclusions

Rapidly solidified glassy ribbons were processed, and based on their thermal characteristics, the theoretical critical thickness (Z_C) was obtained. The estimated Z_C of the two new compositions with a higher Cr content were lower than those estimated by Cheney and Vecchio[11]. Furthermore, the critical thickness (Zc) was obtained experimentally using the wedge-shaped casting method, however this value of Zc was much lower than the one estimated theoretically. Furthermore, the GFA ranking among the three compositions studied here was established experimentally and is in agreement with that predicted theoretically, which foresaw that GFA decreases when the Cr percentage is increased. The glass forming ability of $Fe_{58}Cr_{10}Nb_8B_{24}$, with a fully amorphous bulk sample which was around 0.6 mm thick according to the DRX analysis (estimated theoretically as high as 3.56 mm), offers a good prospect for a new Fe-based glass former alloy with improved corrosion resistance compared with the already reported $Fe_{60}Cr_8Nb_8B_{24}$ alloy.

5. Acknowledgements

The authors would like to thank FAPESP (Projeto Temático n. 2013/05987-8) and CNPq for the financial support. The authors would also like to thank Mr. Filipe Belandrino Swerts and Mr. Victor Felipe Moscoso Linares for their help in processing the samples.

6. References

1. Suryanarayana C, Inoue A. Iron-based bulk metallic glasses. *International Materials Reviews*. 2013;58(3):131-166.

2. Archer MD, Corke CC, Harji BH. The electrochemical properties of metallic glasses. *Electrochimica Acta*. 1987;32(1):13-26.

3. Wang SL, Li HX, Zhang HF, Yi S. Effects of Cr contents in Fe-based bulk metallic glasses on the glass forming ability and the corrosion resistance. *Materials Chemistry and Physics*. 2009;113(2-3):878-883.

4. Pang SJ, Zhang T, Asami K, Inoue A. Bulk glassy Fe–Cr–Mo–C–B alloys with high corrosion resistance. *Corrosion Science*. 2002;44(8):1847-1856.

5. Pang SJ, Zhang T, Asami K, Inoue A. Synthesis of Fe–Cr–Mo–C–B–P bulk metallic glasses with high corrosion resistance. *Acta Materialia*. 2002;50(3):489-497.

6. Jayaraj J, Kim KB, Ahn HS, Fleury E. Corrosion mechanism of N-containing Fe–Cr–Mo–Y–C–B bulk amorphous alloys in highly concentrated HCl solution. *Materials Science and Engineering: A*. 2007;449-451:517-520.

7. Bakare MS, Voisey KT, Chokethawai K, McCartney DG. Corrosion behaviour of crystalline and amorphous forms of the glass forming alloy $Fe_{43}Cr_{16}Mo_{16}C_{15}B_{10}$. *Journal of Alloys and Compounds*. 2012;527:210-218.

8. Ni HS, Liu XH, Chang XC, Hou WL, Liu W, Wang JQ. High performance amorphous steel coating prepared by HVOF thermal spraying. *Journal of Alloys and Compounds*. 2009;467(1-2):163-167.

9. Kiminami CS, Souza CAC, Bonavina LF, de Andrade Lima LRP, Suriñach S, Baró MD, et al. Partial crystallization and corrosion resistance of amorphous Fe-Cr-M-B (M = Mo, Nb) alloys. *Journal of Non-Crystalline Solids*. 2010;356(44-49):2651-2657.

10. Souza CAC, Bolfarini C, Botta Jr. WJ, de Andrade Lima LRP, Falcão de Oliveira M, Kiminami CS. Corrosion resistance and glass forming ability of $Fe_{47}Co_7Cr_{15}M_9Si_5B_{15}Y_2$ (M=Mo, Nb) amorphous alloys. *Materials Research*. 2013;16(6):1294-1298.

11. Cheney J, Vecchio K. Development of quaternary Fe-based bulk metallic glasses. *Materials Science and Engineering A*. 2008;492(1-2):230-235.

12. Marcus M, Turnbull D. On the correlation between glass-forming tendency and liquidus temperature in metallic alloys. *Materials Science and Engineering*. 1976;23(2-3):211-214.

13. Lu ZP, Liu CT. A new glass-forming ability criterion for bulk metallic glasses. *Acta Materialia*. 2002;50(13):3501-3512.

14. Takeuchi A, Inoue A. Mixing enthalpy of liquid phase calculated by miedema's scheme and approximated with sub-regular solution model for assessing forming ability of amorphous and glassy alloys. *Intermetallics*. 2010;18(9):1779-1789.

15. Sanders WS, Warner JS, Miracle DB. Stability of Al-rich glasses in the Al–La–Ni system. *Intermetallics*. 2006;14(3):348-351.